12th International Symposium on Turbulence and Shear Flow Phenomena (TSFP12)
Osaka, Japan (Online), July 19-22, 2022

EFFECT OF BOUNDARY-LAYER TRIPPING ON TRANSONIC BUFFET FOR A LAMINAR-FLOW WING SECTION

Pradeep Moise
Aerodynamics and Flight Mechanics Group
University of Southampton
Southampton, Hampshire, SO17 1BJ, UK
pradeep890@gmail.com

Markus Zauner
Aerodynamics and Flight Mechanics Group
University of Southampton
Southampton, Hampshire, SO17 1BJ, UK
m.zauner@soton.ac.uk

Neil D. Sandham
Aerodynamics and Flight Mechanics Group
University of Southampton
Southampton, Hampshire, SO17 1BJ, UK
n.sandham@soton.ac.uk

ABSTRACT

Transonic buffet refers to the self-sustained periodic oscillations that can occur in transonic flows over wings and is generally associated with strong shock wave/boundary layer interactions. Since it can cause large variations in lift and limit the flight envelope of aircraft, it has been studied extensively. Some studies have classified transonic buffet as either a laminar or a turbulent buffet based on the boundary layer characteristics at the foot of the shock wave and suggested that the mechanisms underlying the two are different. In a recent study (Moise *et al.*, 2021), we have shown by performing wall-resolved Large-Eddy Simulations (LES) of laminar buffet that the features of this type resemble those reported for turbulent buffet, albeit under different flow conditions. In the present study, we present LES of both types of buffet for similar flow conditions, allowing a direct comparison. Turbulent buffet is achieved by forcing boundary layer transition well upstream of the shock foot. These results are compared with those for laminar buffet obtained at the same flow conditions (without enforcing transition). It is shown that unlike the free-transition case, where multiple shock waves exist, there is only a single shock wave when the boundary layer is tripped. Furthermore, for the flow conditions studied, buffet amplitude is significantly reduced for turbulent buffet. However, the buffet frequency remains approximately the same suggesting that mechanisms for both types are similar. This is further corroborated by a spectral proper orthogonal decomposition which shows that buffet and other dynamical characteristics for the two types are consistent.

INTRODUCTION

Self-sustained periodic oscillations that occur in transonic flows over wings under certain flow conditions are associated with a phenomenon referred to as transonic buffet (Helmut, 1974). Transonic buffet, which will also be referred to here as simply 'buffet', can lead to large variations in lift, possibly due to large-scale streamwise motion of shock waves and the periodic separation and reattachment of the boundary layer (BL). This variation in lift, in turn, can lead to passenger discomfort, issues in aircraft control, structural fatigue and even failure (Lee, 2001). Thus, transonic buffet is detrimental to aircraft performance and manoeuvrability and for these reasons, it has been extensively studied with a focus on understanding and controlling its occurrence (Giannelis *et al.*, 2017).

Based on the BL characteristics at the foot of the shock wave, transonic buffet has been classified as either laminar or turbulent buffet (Brion *et al.*, 2020). Turbulent buffet is characterised by the BL developing on the aerofoil's suction surface transitioning to turbulence well upstream of any shock waves present in the flow field. It has been extensively studied and has been shown to occur due to a global instability (Crouch *et al.*, 2007, 2019; Timme, 2020), but the physical mechanisms that drive the instability remain unclear. By contrast, for laminar buffet (where the BL remains laminar from the leading edge to the shock foot) it has been proposed in Dandois *et al.* (2018) that the mechanism sustaining it is different and associated with a bubble-breathing phenomenon. However, in our recent study (Moise *et al.*, 2021), we have shown using numerical simulations and a modal reconstruction that laminar buffet has characteristics that are essentially similar to those reported in previous literature for turbulent buffet. Furthermore, we have shown that bubble breathing occurs due to a high-frequency phenomenon related to vortex shedding similar to those reported in the resolvent analysis performed in (Sartor *et al.*, 2015). We have shown that this is distinct from buffet, but can accompany it.

Simulations in Moise *et al.* (2021) were carried out only for laminar buffet. Here, we further explore the buffet types by performing Large-Eddy Simulations of turbulent buffet for conditions similar to those at which laminar buffet is observed by forcing transition of the BL to turbulence. To achieve transition, we use a trip that is located on the surface of the aerofoil which is modelled by a synthetic, unsteady, wall-normal jet that perturbs the BL. The simulations results are analysed using various tools including spectral proper orthogonal decomposition (Towne *et al.*, 2018) and a flow reconstruction based on the same so as to make direct comparisons between laminar and turbulent types of transonic buffet.

METHODOLOGY

Large-Eddy Simulations, spectral proper orthogonal decomposition and a modal reconstruction based on the latter are employed in this study. Unless otherwise mentioned, the methodology adopted here is the same as that detailed in Moise *et al.* (2021). The major aspects of the latter study are highlighted here for completeness. Two types of simulations are performed, the first being the free-transition case, where the BL transitions naturally (i.e., same as Moise *et al.*, 2021) and a forced-transition case where a trip is introduced.

The in-house flow solver SBLI is used to perform the simulations on transonic buffet. It has been used in a number of previous studies to examine laminar buffet (Zauner *et al.*, 2019; Zauner & Sandham, 2020*b*,*c*; Moise *et al.*, 2021). The compressible Navier-Stokes equations are solved in a dimensionless form with the the required scales being the aerofoil chord, the freestream density, velocity and temperature. For spatial discretisation, a fourth-order finite difference scheme is employed, while a third-order Runge-Kutta scheme is used for time discretisation. A total variation diminishing scheme is employed to capture shock wave features. A spectral-error based implicit LES approach is adopted (Jacobs *et al.*, 2018; Zauner & Sandham, 2020*a*). This has been previously validated against Direct Numerical Simulations for flows where buffet is observed (Zauner & Sandham, 2020*c*).

The aerofoil chosen is Dassault Aviation's laminar, supercritical V2C profile with a blunt trailing edge of thickness 0.5% chord. Multi-block structured grids (C-H type) were generated for each incidence angle using an in-house, open-source code (Zauner & Sandham, 2018). The C-shaped block is of radius 7.5 while the other blocks have a streamwise length of 4.5. The aerofoil is extruded in the spanwise direction with a uniform grid spacing of 5×10^{-4} (see grid-convergence studies) and 1×10^{-3} for the cases of tripped and free transition, respectively. The span is chosen for both cases as 5% of the aerofoil chord based on previous studies (Zauner & Sandham, 2020*c*). The spanwise direction is denoted by z, while the streamwise and the third orthogonal Cartesian direction are labelled as x and y, respectively. The curvilinear circumferential and radial directions are ξ and η. The chordwise direction is referred to as x'.

Zonal characteristic boundary conditions (associated with a buffer zone) are applied at the outflow boundary, while integral characteristic boundary conditions are applied on other outer boundaries (see Moise *et al.*, 2021, figure 1a). The spanwise direction is chosen as periodic. The aerofoil is treated as an isothermal and no-slip wall, except at the location of the trip. Typical grid features in the vicinity of the aerofoil are shown in Fig. 1 (only every 15$^{\text{th}}$ point shown for clarity). The different colours used for grid lines indicate different blocks while the green circle is centred about the tripping location. The grid refinement downstream of the trip was determined such that the turbulent BL features are appropriately captured *a posteriori*, with the grid spacing on the aerofoil surface in wall units being $\delta\xi^+\approx15$, $\delta\eta^+\approx1$ and $\delta z^+\approx10$. The dimensionless time step was chosen as $\delta t=3.2\times10^{-5}$.

Turbulent buffet can occur when the Reynolds number (based on aerofoil chord and freestream velocity) is sufficiently high and other conditions are conducive for natural transition to occur close to the leading edge (*e.g.* Lee, 1989) or when the BL is forced to transition to turbulence in experiments (*e.g.*, using trips, Brion *et al.*, 2020) or numerical studies (*e.g.* Xiao *et al.*, 2006; Garbaruk *et al.*, 2021). Here, due to the moderate values of Reynolds numbers studied, we adopt a synthetic jet which forces transition at a streamwise position, x_t.

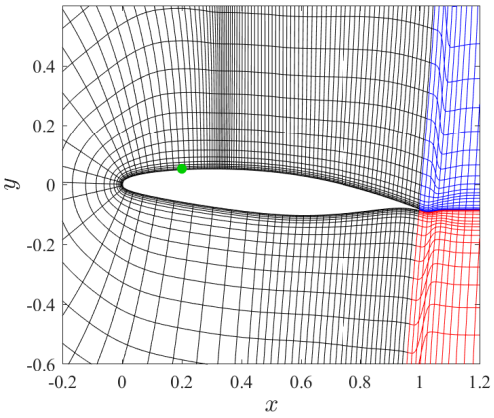

Figure 1. Grid features in the vicinity of the V2C aerofoil (every 15$^{\text{th}}$ point). The green circle shows tripping location.

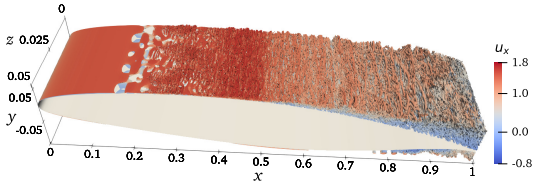

Figure 2. Isosurfaces based on the $Q-$criterion at an arbitrary time instant for the case $M=0.735$, forced transition.

The wall-normal momentum component of the jet is given by

$$\rho u_\eta\,|_{\eta=0}=\sum_{i=1}^{n}A\exp\left(-\frac{(x-x_t)^2}{2\sigma^2}\right)\sin(k_i^2z)\sin(\omega_i t+\phi_i) \tag{1}$$

where ρ is the density and u_η, the wall-normal velocity. The variation in the streamwise direction is that of a Gaussian with amplitude, $A=0.05$, centred about $x_t=0.2$, the streamwise trip position on the aerofoil surface, with a standard deviation, $\sigma=0.00833$. The variation in time and spanwise directions are sinusoidal, with three modes superposed (*i.e.*, $n=3$), with spanwise wavenumbers, $k=\{120\pi,160\pi,160\pi\}$ and angular frequency, $\omega=\{26,88,200\}$ and temporal phase $\phi=\{0,\pi,-\pi/2\}$. The spanwise wavenumbers and amplitude were chosen based on results from the free-transition case such that the former is approximately 10 times the BL thickness at x_t and the latter is a third of the velocity at the edge of the BL, while other parameters were found by trial-and-error.

The effect of forcing transition is shown in figure 2 using isosurfaces of $Q_{\text{inc}}=||\Omega||_2^2-||\mathbf{S}||_2^2=100$. Here, Q_{inc} is the incompressible version of the second invariant of the velocity gradient tensor, while $\mathbf{S}$ and Ω are the rotation and strain-rate tensors, respectively, and $||.||_2$ denotes the second norm. The isosurfaces essentially highlight the regions where rotation dominates over shear strain. This $Q-$criterion (Hunt *et al.*, 1988) implies the presence of vortices and indicates that fluid elements are locally revolving/swirling about some axis. The presence of vortices of varying length scales formed downstream of the trip location ($x_t=0.2$) suggests that by $x\approx0.3$ the BL is fully turbulent. The isosurfaces in the figure are coloured by the local axial velocity, and it can be inferred from the sudden reduction in velocity at $x\approx0.5$ that a shock wave exists well-downstream of the transition location, as shown in the following sections (*e.g.*, see Fig. 5). This indicates that

turbulent buffet occurs for the forced-transition case.

The Reynolds number (based on chord and freestream velocity) and the incidence angle are fixed at $Re = 5 \times 10^5$ and $\alpha = 5^\circ$, respectively. The parameters that are varied are the freestream Mach number, M, and the transition type, with $M = 0.7$ and $M = 0.735$ examined for both free- and forced-transition cases. Additionally, the fluid is assumed to be a perfect gas with a specific heat ratio, $\gamma = 1.4$ satisfying Fourier's law of heat conduction with Prandtl number, $Pr = 0.72$. It is also assumed to be Newtonian and satisfying the Sutherland's law, with the Sutherland coefficient, $C_{\text{Suth}} = 110.4/268.67 \approx 0.41$.

Spatio-temporally coherent structures in the flow field can be extracted using a spectral proper orthogonal decomposition or SPOD (Lumley, 1970; Towne *et al.*, 2018). Here, we use the streaming algorithm and the numerical code provided in Schmidt & Towne (2019) to perform SPOD. This approach solves the eigenvalue problem

$$\int_\Omega \mathbf{S}(\mathbf{x_1}, \mathbf{x_2}, St_0)\, \mathbf{W}(\mathbf{x_2})\, \psi_i(\mathbf{x_2}, St_0) d\mathbf{x_2} = \lambda_i \psi_i(\mathbf{x_1}, St_0) \quad (2)$$

where $\psi_i(\mathbf{x}, St_0)$ and λ_i are the $i-$th eigenfunction (or SPOD mode) and eigenvalue, respectively, of the cross-spectral density tensor, $\mathbf{S}(\mathbf{x}, \mathbf{x}', St_0)$, at a given Strouhal number (dimensionless frequency based on chord and freestream velocity), St_0. Here, $\mathbf{S}$ was computed based on spatio-temporal data collected on a two-dimensional plane, $z = 0$ (with $\mathbf{x}$ and $\mathbf{x}'$ being any two points on the plane), while $\mathbf{W}$ is the weight matrix associated with the quadrature on the grid (a weighted 2-norm). The eigenvalues are indexed such that $\lambda_1 > \lambda_2 > \lambda_3 ...$, implying that most-energetic SPOD mode is $\psi_\mathbf{1}$ with higher indices representing modes of lower energies. The energy content of modes other than $\psi_\mathbf{1}$ were negligible (not shown) and thus, these modes were not considered. The temporal data at various grid points was sampled at $F_s = 12.5$ (based on chord and freestream velocity and about two orders of magnitude higher than observed buffet frequencies) for a duration of 70 dimensionless time units ($\approx$ 10 buffet cycles). These were then divided into blocks of total time, $T_\zeta = 44$ and $\mathbf{S}$ was computed using the Welch's method with 50% overlap.

The flow field data, $\mathbf{q}(\mathbf{x}, t)$, was decomposed using SPOD and buffet features were isolated by finding $\psi_\mathbf{1}(\mathbf{x}, St_b)$, where St_b is the buffet frequency. Note that this SPOD mode is associated with the most dominant coherent motion present in the flow field. The reconstructed flow field based on only the buffet mode is then obtained by combining the spatio-temporal features of this SPOD mode with the mean flow field, $\overline{\mathbf{q}}$ (see Moise *et al.*, 2021, for further details) and is given by

$$\tilde{\mathbf{q}}(\mathbf{x}, t) = \overline{\mathbf{q}}(\mathbf{x}, t) + \text{Re}\left\{\sqrt{\lambda_i}\psi_i(\mathbf{x}, St_b) \exp\left(2\pi \text{i} St_b t\right)\right\} \quad (3)$$

Grid-convergence studies

Studies examining the effect of the grid were performed for the forced-transition case (free-transition cases have been examined in Zauner *et al.*, 2019). The grid spacing in different directions (x, y and z) was varied independently. It was observed that the solutions were most sensitive to the spatial resolution in the $z-$direction. A comparison of the mean pressure coefficient for $M = 0.735$, $Re = 5 \times 10^5$ and $\alpha = 5^\circ$ when the grid spacing in the spanwise direction is varied is shown in Fig. 3. The solutions for the lowest resolution is found to be inadequate, with the mean shock wave position being further

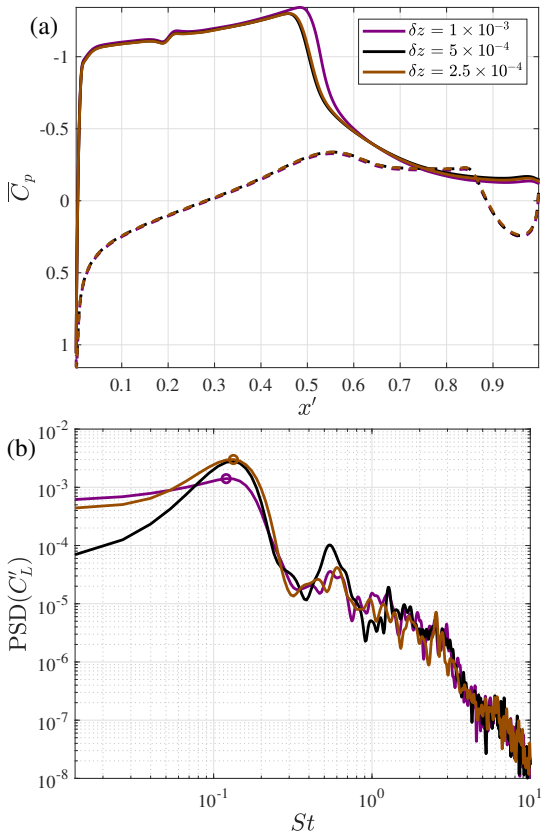

Figure 3. Comparisons of (a) time- and span-averaged pressure coefficient variation on the aerofoil surface (dashed curves: pressure surface) and (b) power spectral density of lift fluctuations for various choices of spanwise grid spacing.

downstream and buffet amplitude (circles) reduced, but for the other two cases these features and buffet frequency match adequately. Thus, $\delta z = 5 \times 10^4$ was used in all other simulations.

RESULTS

The temporal variation of the span-averaged lift coefficient, C_L, for time past transients ($t > t_0$) for the free- and forced- transition cases are compared in figure 4*a* for different M. The power spectral density (PSD) of the fluctuating component of C_L is compared in figure 4*b*. Strong lift oscillations, characteristic of buffet, can be seen for the free-transition cases with a peak observed in the PSD at $St_b = 0.09$ and 0.16 for $M = 0.7$ and $M = 0.735$, respectively (highlighted by circles). The oscillations are significantly subdued when transition is forced. At $M = 0.7$, no clear lift oscillations or a peak in the PSD are discernible, while at $M = 0.735$, the PSD(C_L') associated with buffet drops by almost two orders of magnitude, with $St_b = 0.13$. Thus, in the parameter range studied, it appears that forcing BL transition leads to the suppression or reduction in strength of buffet when compared to free transition. This suggests two possibilities: (i) buffet amplitude at any flow condition (*i.e.*, M, α and Re) might be reduced or (ii) buffet onset might be shifted to higher α for forced-transition cases. The latter implies that at higher α, there might be relatively higher buffet amplitudes for the forced-transition cases. This is not further explored here. Another important aspect seen here is that the buffet frequency remains approximately the same for both free- and forced-transition cases, which corroborates with the proposition in Moise *et al.* (2021) that laminar and turbu-

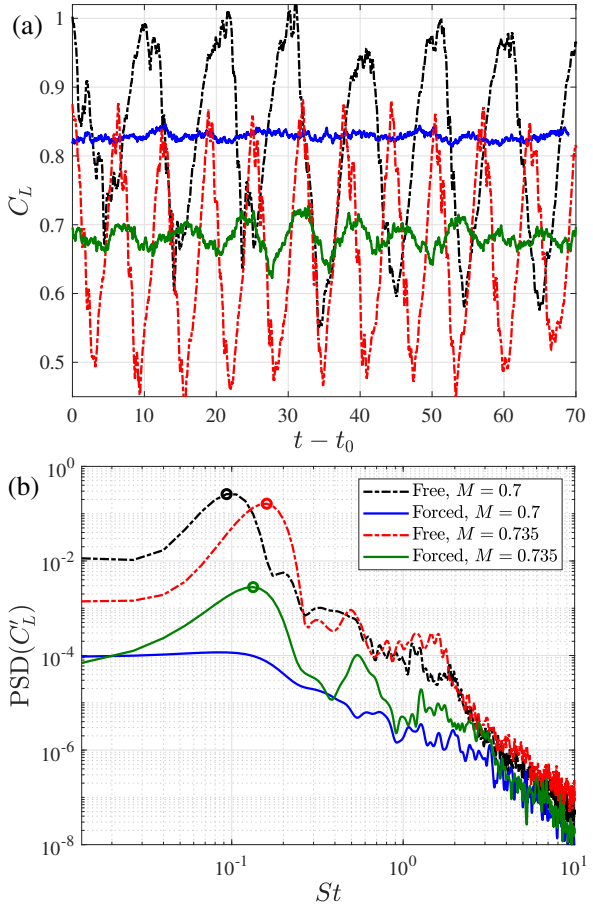

Figure 4. (a) Temporal variation of the lift coefficient, C_L, past transients and (b) the power spectral density of its fluctuating component for different M.

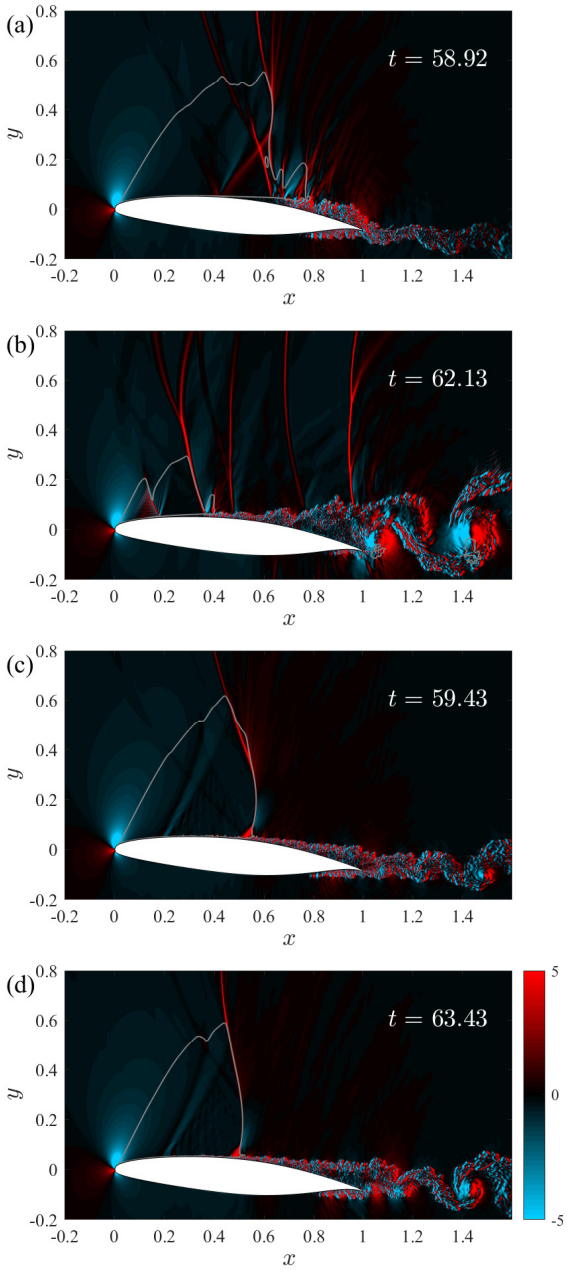

Figure 5. Density-gradient contours at high- (a,c) and low-lift (b,d) phases for the free- (a,b) and forced-transition (c,d) cases for $M = 0.735$.

lent buffet have similar mechanisms. This should be contrasted with the bubble-breathing phenomenon reported in Dandois *et al.* (2018) which occurs at a frequency an order of magnitude higher ($St \approx 1$). From Fig. 4*a*, it can also be inferred from the temporal variations that the time-averaged C_L is approximately the same at a given M for both free- and forced-transition cases. Another interesting feature is the presence of bumps in the PSD at an intermediate frequency of $St \approx 0.5$ and a high frequency $St \approx 1$ for both cases at $M = 0.735$. The latter will be shown to occur due to wake modes reported in Moise *et al.* (2021).

Instantaneous contours of the streamwise density gradient are plotted in Fig. 5 for both free- and forced-transition cases for $M = 0.735$ at approximate times when the lift achieves a local maximum or minimum. Multiple shock waves, characteristic of laminar buffet at low Re (Ackeret *et al.*, 1947; Zauner *et al.*, 2021), are observed for the free-transition case (a,b), while the envelope of the supersonic region delineated by the sonic line (grey curve), varies significantly with time. By contrast, only a single shock wave is present for the forced-transition case (as is commonly reported in literature) and the streamwise excursions of the shock are relatively low. Note that the shock position, $x_s \approx 0.5$, which is well downstream of x_t implying turbulent buffet. Thus, buffet amplitude at moderate Re is shown to be sensitive to the BL characteristics upstream of the shock wave. These findings align with the global linear stability analysis results in Garbaruk *et al.* (2021), where a buffet mode becomes unstable at lower α when the BL is tripped further downstream. This suggests that for a constant α, buffet intensity would increase with an increase in streamwise extent of the laminar BL. Comparing the wake of the aerofoil at the low-lift phase (b,d) with that at the high-lift phase (a,c), we see that for both free and forced transition, we have a stronger vortical organisation resembling the von Kármán vortex street.

SPECTRAL PROPER ORTHOGONAL DECOMPOSITION

The eigenvalue spectra based on the dominant eigenvalue, λ_1, for both forced- and free-transition cases are shown in Fig. 6. The peaks at low-frequency (highlighted by circles) match the buffet frequency seen for the lift coefficient. Since the intermediate frequency occurs close to the harmonic of the buffet mode and since no clear peak is present in the SPOD spectra it

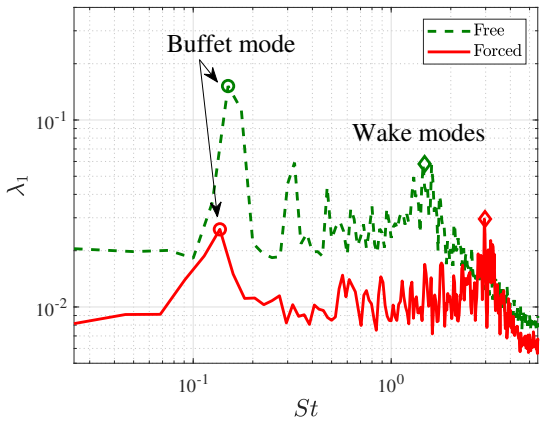

Figure 6. The eigenvalue spectra of the dominant eigenvalue from SPOD for free and forced transition at $M = 0.735$.

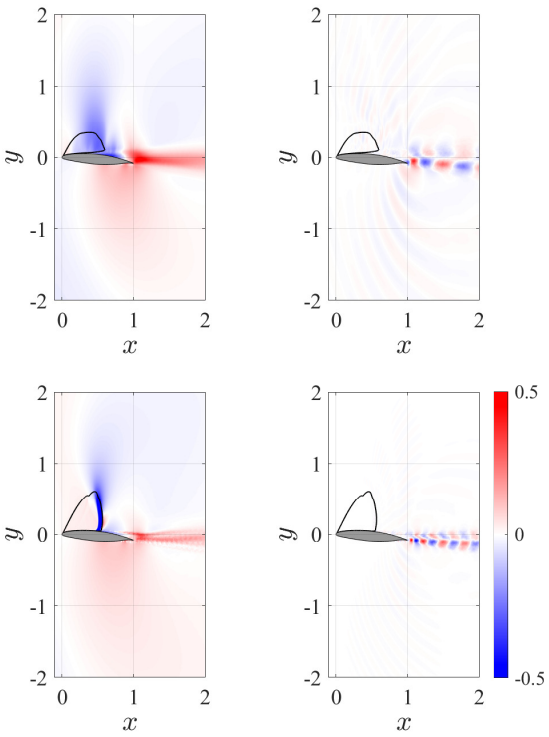

Figure 7. Contours of density of the buffet (left) and wake (right) modes for the free-transition (top) and forced-transition (bottom) cases for $M = 0.735$. The sonic line based on time-averaged flow is shown using the black curve.

is not studied here. Bumps in the spectra in the high-frequency range of $St \sim O(1)$ (largest amplitude in the range highlighted by a diamond) are discernible and are related to vortex shedding, as shown next.

The contours based on the real part of the density field of the buffet mode and the most-dominant wake mode obtained in SPOD are shown in Fig. 7 for the two cases. The wake modes for both cases show a clear von-Kármán vortex street pattern, with the vortical length scale being larger for the free-transition case. The buffet modes for the two cases also have a similar flow structure. For example, the contours indicate that when a reduction in density from the mean value occurs on most parts of the suction surface (blue regions), the density in the wake of the aerofoil increases above the mean

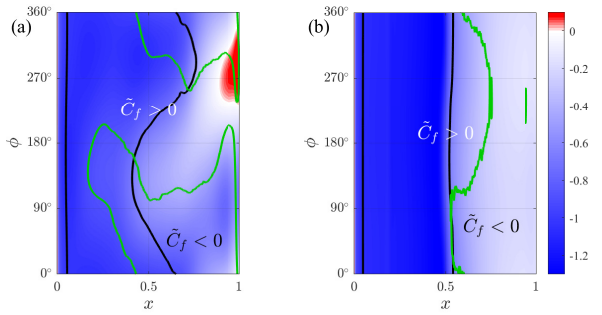

Figure 8. Spatio-temporal contours of $\tilde{C}_p$ for the cases of (a) free and (b) forced transition. The isolines for $\tilde{M}_{\text{loc}} = 1$ (solid black curve) and $\tilde{C}_f = 0$ (solid green curve) are also overlaid.

value (red contours), implying that these two regions are out of phase in a buffet cycle. Similarly, the maximum reduction occurs approximately at the mean shock wave position (black curve). Other minor differences between the free- and forced-transition cases can be accounted for by the presence of multiple shock waves and a larger buffet amplitude for the former case. Note that multiple shock waves were observed for free-transition cases even in the absence of buffet (see $M = 0.69$ case in Moise *et al.*, 2021) implying that these are features of low-Reynolds number flows and are not related to buffet (Zauner *et al.*, 2021). Also, the unstable mode associated with buffet obtained through global linear stability analysis of solutions of steady Reynolds-Averaged Navier Stokes equations in other studies have a striking resemblance to the buffet mode for the forced-transition case seen here (*e.g.*, compare Fig. 7 bottom left in present study with density contours shown in Fig. 12, Sartor *et al.*, 2015). Together, these results indicate that the origins of laminar and turbulent buffet are the same.

To understand the associations between shock wave and BL separation in buffet, a flow reconstruction based only on the buffet mode and the mean flow field (see Eq. 3) is examined. A spatio-temporal diagram showing contours of the pressure coefficient on the aerofoil surface, $\tilde{C}_p$, along with the curves delineating separated-flow regions (*i.e.*, skin-friction coefficient, $\tilde{C}_f = 0$) and the sonic line (*i.e.*, $\tilde{M}_{\text{loc}} = 1$, based on the local flow field at a distance 0.5 from the aerofoil surface) are compared in Fig. 8. Here, '$\sim$' denotes a reconstructed quantity, while ϕ denotes the phase based on a single buffet cycle, with $\phi = 0^\circ$ and 180° denoting the low-lift and high-lift phases, respectively. The variations of $\tilde{C}_p$ are more gradual for the free-transition case, which is expected due to the multiple unsteady shock waves present in the LES field. By contrast, the pressure jump is abrupt for the forced-transition case. Also, for the former case, the upstream motion of the shock wave is characterised by large flow separation (approximately, $0^\circ \leq \phi \leq 150^\circ$), while the flow remains fully attached when the shock moves downstream. By contrast, for the latter case, the flow is mostly separated downstream of the shock. However, the motion of the separation point in different phases of the cycle is similar for both cases and the differences seem to be due to stronger shock motion for the free-transition case as compared to the forced-transition case. This is especially seen when considering the qualitative variation of the isoline $\tilde{C}_f = 0$ (green curves).

CONCLUSION

Wall-resolved Large-Eddy Simulations of laminar and turbulent transonic buffet are performed. The latter is achieved by forcing transition using a wall-normal jet on the aerofoil surface well-upstream of the shock wave. Simulations for this forced-transition case were performed for the same flow conditions under which laminar buffet occurs when boundary layer transition is instead allowed to occur naturally (free-transition case). The flow conditions chosen are a Reynolds number (based on freestream velocity and aerofoil chord) of $Re = 500,000$, an incidence angle, $\alpha = 5^\circ$, for two different freestream Mach numbers of $M = 0.7$ and 0.735. It was observed that when transition is forced, buffet is eliminated ($M = 0.7$) or reduced in amplitude ($M = 0.735$) as compared to the corresponding free-transition case. Also, a single shock wave was present when the transition is forced, while multiple shock waves were observed for the free-transition cases, which agrees with results from Ackeret *et al.* (1947). However, the dynamics of the system seem to be similar for both free- and forced-transition cases. For example, the frequency for the two are the same when buffet occurs. Similarly, a spectral proper orthogonal decomposition showed that the flow is dominated by modes at two different frequencies. The lowest-frequency mode was identified as due to buffet and comparisons between free- and forced-transition cases showed that, when the variations in buffet amplitude is accounted for, the features of the modes were essentially similar. This study provides further evidence that laminar and turbulent buffet have the same origins. Importantly, this study links the turbulent buffet features at high Reynolds numbers ($Re > 10^6$) reported in literature (*e.g.* Sartor *et al.*, 2015) and laminar buffet features reported at moderate Reynolds numbers of $Re \sim O(10^5)$ (*e.g.*, Zauner & Sandham, 2020*c*; Moise *et al.*, 2021).

Acknowledgement This work was carried out through computational time provided by UK Turbulence Consortium through the EPSRC grant EP/R029326/1 and funding from the EPSRC grant EP/R037167/1. We also acknowledge the use of ARCHER2 (UK national supercomputing facility) and the IRIDIS High Performance Computing Facility (University of Southampton), and associated support services, in the completion of this study. The V2C airofoil geometry was kindly provided by Dassault Aviation.

REFERENCES

Ackeret, J, Feldmann, F & Rott, N 1947 Investigations of compression shocks and boundary layers in gases moving at high speed. *Tech. Rep.* TM 1113. NACA.

Brion, V, Dandois, J, Mayer, R, Reijasse, P, Lutz, T & Jacquin, L 2020 Laminar buffet and flow control. *Proc. Inst. Mech. Eng. Part G J. Aerosp. Eng.* **234** (1), 124–139.

Crouch, J. D, Garbaruk, A & Magidov, D 2007 Predicting the onset of flow unsteadiness based on global instability. *J. Comput. Phys.* **224** (2), 924–940.

Crouch, J. D, Garbaruk, A & Strelets, M 2019 Global instability in the onset of transonic-wing buffet. *J. Fluid Mech.* **881**, 3–22.

Dandois, J, Mary, I & Brion, V 2018 Large-eddy simulation of laminar transonic buffet. *J. Fluid Mech.* **850**, 156–178.

Garbaruk, A, Strelets, M & Crouch, J. D 2021 Effects of Extended Laminar Flow on Wing Buffet-Onset Characteristics. *AIAA J.* **59** (8), 1–7.

Giannelis, N. F, Vio, G. A & Levinski, O 2017 A review of recent developments in the understanding of transonic shock buffet. *Prog. Aerosp. Sci.* **92**, 39–84.

Helmut, J 1974 Critical review of methods to predict the buffet capability of an aircraft. *Tech. Rep.* 623. AGARD.

Hunt, J. C. R, Wray, A. A & Moin, P 1988 Eddies, streams, and convergence zones in turbulent flows. In *Center for Turbulence Research Proceedings of the Summer Program 1988*.

Jacobs, C. T, Zauner, M, De Tullio, N, Jammy, S. P, Lusher, D. J & Sandham, N. D 2018 An error indicator for finite difference methods using spectral techniques with application to aerofoil simulation. *Comput. Fluids* **168**, 67–72.

Lee, B. H. K 1989 Investigation of flow separation on a supercritical airfoil. *J. Aircr.* **26** (11), 1032–1037.

Lee, B. H. K 2001 Self-sustained shock oscillations on airfoils at transonic speeds. *Prog. Aerosp. Sci.* **37** (2), 147–196.

Lumley, J. L 1970 *Stochastic tools in turbulence*, 1st edn. Academic Press.

Moise, P, Zauner, M & Sandham, N 2021 Large eddy simulations and modal reconstruction of laminar transonic buffet. arXiv:2110.13237 [physics.flu-dyn], accepted, *J. Fluid Mech.*

Sartor, F, Mettot, C & Sipp, D 2015 Stability, receptivity, and sensitivity analyses of buffeting transonic flow over a profile. *AIAA J.* **53** (7), 1980–1993.

Schmidt, O. T & Towne, A 2019 An efficient streaming algorithm for spectral proper orthogonal decomposition. *Comput. Phys. Comm.* **237**, 98–109.

Timme, S 2020 Global instability of wing shock-buffet onset. *J. Fluid Mech.* **885**, 1–32.

Towne, A, Schmidt, O. T & Colonius, T 2018 Spectral proper orthogonal decomposition and its relationship to dynamic mode decomposition and resolvent analysis. *J. Fluid Mech.* **847**, 821–867.

Xiao, Q, Tsai, H. M & Liu, F 2006 Numerical study of transonic buffet on a supercritical airfoil. *AIAA J.* **44** (3), 620–628.

Zauner, M, De Tullio, N & Sandham, N. D 2019 Direct numerical simulations of transonic flow around an airfoil at moderate reynolds numbers. *AIAA J.* **57** (2), 597–607.

Zauner, M, Renou, A, Dandois, J, Brion, V, Moise, P & Sandham, N 2021 Numerical and experimental analysis of transonic buffet for different airfoil geometries at moderate Reynolds numbers. In *UK Fluids Conference Book of Abstracts*, *UK Fluids Conference* 5, pp. 08A–3.

Zauner, M & Sandham, N. D 2018 Multiblock structured grids for direct numerical simulations of transonic wing sections. *10th Int. Conf. Comput. Fluid Dyn. ICCFD 2018 - Proc.* **10** (2), 1–18.

Zauner, M & Sandham, N. D 2020*a* Les study of the three-dimensional behaviour of unswept wing sections at buffet conditions. In *Direct and Large Eddy Simulation XII* (ed. Manuel García-Villalba, Hans Kuerten & Maria Vittoria Salvetti), pp. 329–334. Cham: Springer International Publishing.

Zauner, M & Sandham, N. D 2020*b* Modal Analysis of a Laminar-Flow Airfoil under Buffet Conditions at Re = 500,000. *Flow, Turbul. Combust.* **104** (2-3), 509–532.

Zauner, M & Sandham, N. D 2020*c* Wide domain simulations of flow over an unswept laminar wing section undergoing transonic buffet. *Phys. Rev. Fluids* **5** (8), 83903.